Volume 10, Issue 3, 2020, 5575 - 5585 ISSN 2069-5837

Biointerface Research in Applied Chemistry

www.BiointerfaceResearch.com

https://doi.org/10.33263/BRIAC103.575585

Original Research Article Open Access Journal

Received: 10.03.2020 / Revised: 20.03.2020 / Accepted: 20.03.2020 / Published on-line: 22.03.2020

An overview on Coronaviruses family from past to Covid-19: introduce some inhibitors as antiviruses from Gillan's plants

Majid Monajjemi [1,*], Fatemeh Mollaamin [1], Shahrokh Shojaei [2]

[1]Department of chemical engineering, Central Tehran Branch, Islamic Azad University, Tehran, Iran
[2]Department of biomedical engineering, Central Tehran Branch, Islamic Azad University, Tehran, Iran
*corresponding author e-mail address: ***maj.monajjemi@iauctb.ac.ir*** | Scopus ID 6701810683

ABSTRACT

Among the herbal medicine that commonly used in relieving diseases we choose 4 species as the source for active constituents to be examined as its potential as anti SARS-CoV-2, namely Matrine, Cytarabine, Gemcitabine and Vidarabine from which are extracted from Gillan 's plants such as Trshvash, Chuchaq, Cote D'Couto and Khlvash in Iran. The mechanisms by which these agents exercise their antivirus action are calculated via analyzing of NMR and physical chemistry properties via docking. The drugs which are discussed in this article, some of them are in pre-clinical trials or clinical development and some are available in market such as Matrine, Cytarabine, Gemcitabine and Vidarabine. In this work, we have optimized and discussed about several active compounds which are extracted from famous plants through NMR study. These data in high-accuracy determine for anti-SARS-CoV-NSPs confirm our molecular modelling and also exhibited that Cytarabine, a compound found in Chuchaq, and Matrine from Trshvash, bind to those receptors with lower energies compared to the respected reference compounds. These finding indicated that both compounds possess better binding interaction and may inhibit the initial virus infection to the host cell

Keywords: *Coronaviruses; SARS-CoV-2; COVID-19; Receptor binding domain(RBD); ACE2 (Angiotensin Converting Enzyme-2); protease domain (PD)*

1. INTRODUCTION

Coronaviruses or subfamily *Corona-virinae* are enveloped, positive-sense m-RNA virus that include the largest known RNA genomes with a length of up to 32 kb. Coronaviruses are important subjects in nowadays for any investigation to help the humanity. Particularly virulent forms have emerged from its natural animal hosts and pose a threat to human communities [1, 2]. In 2003, the SARS virus emerged in China from bat populations, moving to civets and then to humans. 10 years later, the MERS viruses emerged from bats, transferring in the Middle East to dromedary camels and finally to humans. Nowadays, a new family coronaviruses have emerged in China through living animals in the markets. Structural and genetic biological information can help us for understanding these dangerous foes, and hopefully will develop new ways to fight them [3, 4].

Coronaviruses (containing strains) are a family's group of viruses that are known for diseases in mammals and birds. In humans life it is typically spreads through airborne droplets of any fluids produced via infected individuals. Some considerable of these viruses, including SARS-CoV-2 or COVID-19 can cause death in humans. SARS-CoV-2 was first identified and characterized in the Chinese city of Wuhan in 2019 with a mortality rate of around one percent. Coronavirus consist of a genome combined of a large RNA strand (largest of all RNA viruses) and those genomes attack to target like a m-RNA during infect the cells, and direct the synthesis of two large polyproteins where contain the machinery which the viruses need for replicating new viruses[2-4].

The proteins contain a replication/ transcription complexes that make more RNA, various structural proteins, and two proteases. These proteases play important roles to cut the polyproteins inside all of the functional spices. The major section protease of this virus makes most of those cuts. The SARS-CoV-2 (2019-nCoV) which is currently sparking most dangers in "Wuhan" is a dimer of two identical subunits that together form two active sites [5, 6].

Its protein folding is similar to serine proteases such as trypsin and also the cysteine amino acids which perform the protein-cutting reaction close to histidine as extra domain stabilizes [4,7]. These dimers have the peptides-like inhibitors bound in the active sites. Pair proteases from the SARS virus are the main proteases are similar to the Wuhan's virus, including a few splits at eleven sites in the polyproteins.

The papain-like protease (Fig.1) has a unique subunit using cysteine amino acid by the reaction which makes three specific cuts in the SARS polyproteins. Consequently have several slicing proteins in the infected cell. One of the consequences is that through production of interferons in the innate immune systems, causes short-circuiting our defenses against the virus. Researchers potentially using this structure for investigation of the compound that has blocked the proteases action, to apply as antiviral drugs. The variety of coronaviruses exhibits a great challenge with these efforts. Coronaviruses have been characterized into 4 configurations and structural studies have to exhibit which the proteases of those viruses might be very different for any further drug designing. Important way is to try for designing the broad-spectrum inhibitors against the progenitor bat coronavirus [Fig.1], which may then provide a key for discovering related inhibitors for these kind viruses. All subunits of CoV-RNA synthesis machinery include a complex of several non-structural proteins (NSP) that produced viral polyproteins. Many various CoV-NSPs

possess enzyme activities related to RNA modification. After the emergence of SARS-CoV, there were several attempts for characterizing the replication complexes of CoVs . It is notable that firstly the fundamental knowledge about the CoV-RNA synthesis were a predication structural of the NSP- RNA polymerase . This resulted in high-resolution structures determination for many of the SARS-CoV-NSPs in isolation using X-ray crystallography and NMR.

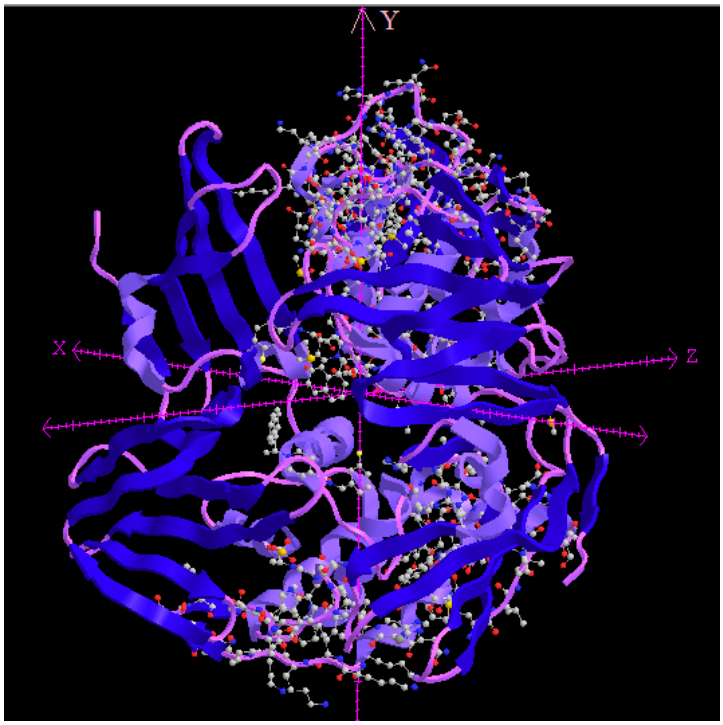

Figure 1. X-Ray Structural and Biological Evaluation of a Series of Potent and Highly Selective Inhibitors of Human Coronavirus Papain-Like Proteases [8].

Their molecular structural were containing information regarding the single N-terminal of the virus polymerases[9-13]. Coronaviruses (CoVs) have been structured via unique-stranded RNA that are associated with a few natural hosts. CoV is partitioned into alpha, beta, gamma and delta categories. Among them the beta group consists of A, B, C, and D subunits (scheme1.)

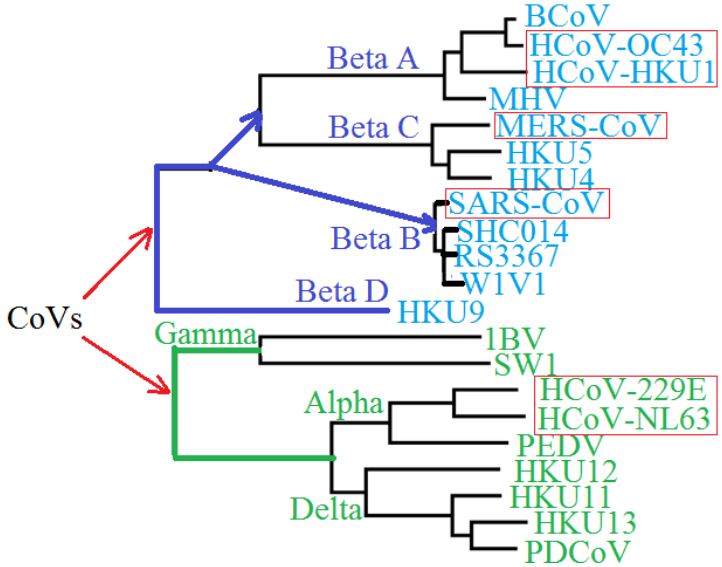

Scheme 1. Schematic trees created with the H-CoVs from all four gen-groups. H-CoVs are denoted in red rectangular frame.

These six H-CoVs are mentioned in red rectangular frame, including (1)-HCoV-229E (229E) and (2)-HCoV-NL63 (NL63) in the alpha group, (3)-HCoV-OC43 (OC43), (4)-HCoV-HKU1 (HKU1) in beta subgroup A, (5)-(SARS-CoV) (severe acute respiratory syndrome)CoV in beta subgroup B, and finally (6)-MERS-CoV (Middle East respiratory syndrome CoV) in beta subgroup C [9-13]. Recently, SARS-CoV and MERS-CoV have been emerged in the human population and caused severe pulmonary disease with alarmingly high case-fatality rates. SARS-CoV infections firstly emerged in China in 2002 which spread rapidly as a global epidemic.

MERS-CoV emerged in Saudi Arabia in 2012 and spread via the Middle East and also in 2015 another type of MERS-CoV appeared in South Korea. By the way, the other common viruses including 229E, OC43, and NL63, generally infect the human upper respiratory tract. In addition they also are responsible for severe and even fatal diseases in children, old people, and immunocompromised patients [11-13]. Among these H-CoVs, which are rapidly evolving, OC43 isolates with novel genomes are being continuously identified [14-16].

The SL-CoV (SARS-like-CoV) and ML-CoV (MERS-like-CoV) also pose a great threat to public health in the world. Recent reviews and research discovered a few types more of SL-CoV, such as SL-WIV1-CoV and SL-SHC014-CoV. These SL-CoVs can be applying the same SARS-CoV receptor to directly enter permissive human cells without the need for adaptation [17]. The SARS-approximately became pandemic, behind disappeared when the quarantine precautions were taken. Moreover, the ML-CoVs, are bat CoV-HKU4, was exhibit for recognizing the MERS-CoVs receptors (Fig. 2) CD-26 and infect human cells, after mutations of S746R with N762A) into its S protein [18].

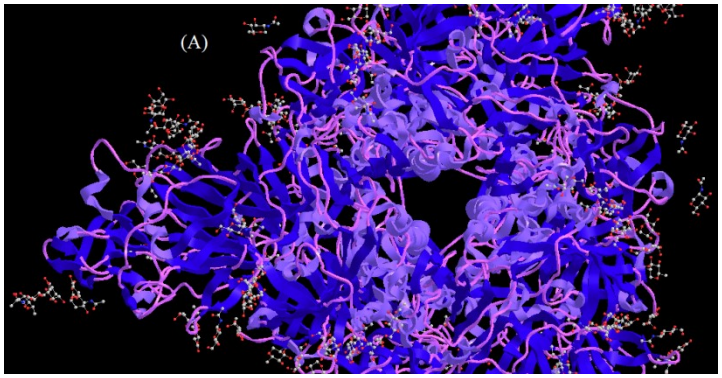

Figure 2. MERS-CoV S structure in complex with sialyllewis-X [19].

Since no anti-HCoVs drugs are currently available for clinical usage, there are incumbent for searching to conserve target site based on properties of HCoV which via the S glycoprotein plays an important role in mediating viral infection. The S-proteins consist of two subunits, S1 and S2 (Fig.3).

Their subfamilies of *Corona-virinae*, that include viruses of both medical and veterinary importance, might be separated into the four genera alpha-, beta-, gamma- and delta-coronavirus (α-, β-, γ- and δ-CoV). The coronavirus particle comprises at least the four canonical structural proteins E (envelope protein), M (membrane protein), N (nucleon-capsid protein), and S (spike protein).

The S1 subunit binds the cellular receptors via their receptors-binding domains, followed via conformational changing

into the S2 subunits (Fig.4), which yields the fusion peptides to insert into the host targets cell membrane.

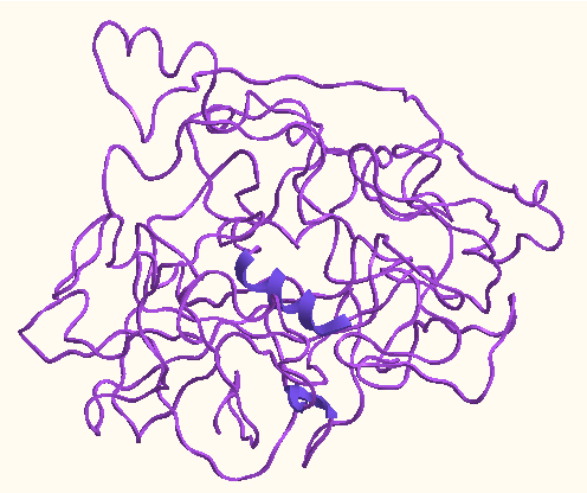

Figure 3. S1 subunit model of H52 strain of IBV coronavirus.

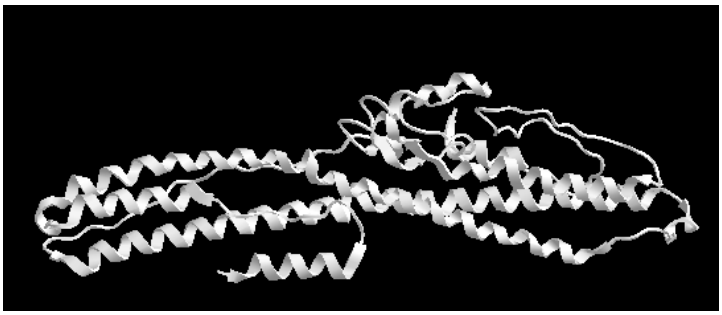

Figure 4. S2 subunit model of SARS Corona virus S protein.

Moreover, these viruses belonging to the "A" lineage of the β-coronaviruses translate the membrane-anchored HE proteins. The "S" glycol-protein includes both the receptor-binding domain (RBD) and the domains twisted in a merger situation. Although each coronavirus belongs to be restricted to one host of a single animal, genome sequencing verifies which CoV has crossed the host species barrier frequently [20].

Obviously, several of humanity coronaviruses seem to originate from bat which transmitted to people through the intermediate hosts which mean similar zoonotic infections will appear in the future. Usually, 4 mechanisms explain cross-species transmission of a particular virus [21] which are (1), the cellular tropism of a virus which can be determined through the susceptibility of host cells (2), the permissiveness of these host cells for allowing the viruses to replicate and to complete its life cycle (3), the accessibility of susceptible and permissive cells in the host (4), the innate immune responses that might be restricted viral replications in the hosts specific manner.

1.1. Structure of the coronavirus s protein and S1, S2 subunit.

Category of "S" proteins are class one (I) of viral fusion proteins[22] same as influenza [23-25], that like other classes (I) can be folded into a meta-stable pre fusion due to its translation.

Size of "S" protein varies among coronaviruses between 1100 - 1600 residue's ranges length (around 220 kilo Dalton). Trimers of the "S" proteins consist of 17–24-nm, and in addition architectural structure decorate the membrane surface of the corona virus particles. "S" proteins are also a major goal for neutralizing antibodies elicited through the immune system of the infected hosts which can be isolated into two functionally distinguished subunits [26]. "S_1"subunit consists of a section as receptor recognition but in contrast "S_1" ,the S_2 subunit can simplifies the membrane fusion for controlling the S proteins into the viral membrane (scheme 2).

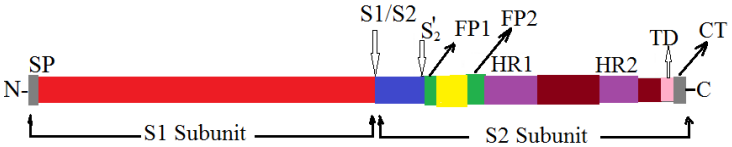

Scheme 2. Schematic position of coronavirus S protein based on domains/sites and signal peptide, two proteolytic cleavage sites (S1/S2 and S'$_2$), two proposed fusion peptides (FP1 and FP2), two heptad repeat regions (HR1 and HR2), transmembrane domain (TD), and cytoplasmic tail (CT).

The S1 and S2 subunits might be divided via a cleavage site which is known by Furin-like proteases when "S" protein bio-genesis in the infected cell. Structures of the spike subunits of two β-coronaviruses including MHV and HCoV-HKU1 has provided novel insights into the architecture of the S trimer in its pre-fusion state [27, 28].

1.1.1. Structure of S1.

The S1 domain of the β-coronaviruses rolls multi architecture that structurally formed to 4 distinguished units including A, B, C and D . Subunits A and B might serve as a RBD

Scheme 3. Schematic representation of MHV spike protein sequence, the S1 domains A, B, C, and D, are colored in green, red, blue and yellow respectively, and the linker region connecting domains A and B in turquoise, the S2 region is colored in violet.

The core segment of unit "A" rolls a galectin-like β- fold, while unit B includes a structurally conserved segment sub unit of non-parallel β-sheets [29, 30]. Domain B is structured with an additional loop on the viral membrane direction which might vary considerably in size among virus of the b β-coronavirus genus related to hyper-variable range. Oligomerization of the "S" protein yields in a nearest trimer cluster of the B subunit of the spike over top of the S2, while the three "A" subunit can be ordered distally of the center. Unlike subunits "A" and "B:, the S1 C-terminal units "C" and "D" are made of of the initial proteins including β-sheets conformation towards the S_2 and divided S_1 subunits which are attached via a few loops. In contrast of the S_2 domain, the S_1 exhibits a small level of amino acids sequences between varies CoVs generation. In addition, S_1 domain differs extremely in sequences length spectrum from 544 (S of bronchitis's viruses) to 944 (S of bat's CoVs), which means a difference in molecular structures and conformational models of the spikes in CoVs generation. Although structural understanding of the spikes γ *and* δ CoVs are currently unknown, two kinds folding have been assigned in the S_1 subunit of α- CoVs . These kinds viruses potentially can interact with host molecules. Structural data are available for the S_1 C-terminal of two α-coronaviruses and S proteins that differ considerably from which of β-CoVs. α- CoVs exhibits a β-sandwich core conformation, while a β-sheet core structures are seen for β-CoVs [31].

1.1.2. Structure of S2.

The S_2 consist of a protein part which streamline the cell fusion of virus. It contains a fusion peptide, 2 heptad repeat range (HR_1 with HR_2) and transmembrane protein which completely conserved among component of corona viruses in different generation. In "MHV" and HKU1, the S proteins and S2 with α-helical structures and non-parallel beta-sheet are located at the viral membrane proximal end. Seventy five angstrom of central helical structure of the HR1 over the entire length of the S2 trimmer is structured as 4- α-helices in the length of the S2 domains [32-34].Fifty five angstrom of long helical S20 cleavage site runs parallel to central helix through hydrophobic interactions. The fusion peptide segment is a small helix of hydrophobic sections that are buried in the interfaces via the other components of S2. The fusion peptide segment is a small helix of hydrophobic sections that are buried in the interfaces via the other components of S2.

In contrast other classes one(I) fusion proteins, the conserved peptides are not HR1 due to residues up-stream of these spectrum (Scheme 2 &3). Recently a report has been published for the existence of another fusion peptide which is known as FP2, in family of HR1 [35]. This HR2 placed near the C-terminal end of the S domain. The distal tip of the S2 trimer connects through a hydrophobic interaction with domain B which consists of the C-terminal section of HR1 [36, 37]. Interactions among these spectrums of the S_2 trimer and subunit B causes to prevent premature structural changing due to the conversion of the S protein towards the stable post-fusion structures. Subunits C and D of the β-CoVs S1 domain connect to subunits A and B via surfaces of the adjacent S2 Domain "A" due to its interaction with the S_2 trimer.

2. MATERIALS AND METHODS

2.1. Isotropic and anisotropic parameters.

The total chemical shielding tensor σ is a non-symmetric tensor which can be separated into three independent parameters: anisotropic, traceless symmetric and traceless anti-symmetric. The spherical tensor has been exhibited by Haeberlen and Mehring. They have investigated fundamental tensors as

$$\zeta_{zz} = (\sigma_{zz} - \sigma_{iso}) = (\sigma_{33} - \sigma_{iso})$$

Where ζ_{zz} is the reduced anisotropy and can be calculated through: the asymmetry shielding (η) can be calculated as: $= \left(\frac{\sigma_{yy}-\sigma_{xx}}{\zeta_{zz}}\right)$.

It is notable that the spin magnetic resonance is seldom isotropic, therefore they have to be represented by new tensors (Herzfeld—Berger notation). These tensors are known as span (Ω), which describe the maximum width of the model and the skew (K) of the tensor being $\Omega = \sigma_{33} - \sigma_{11}$. Moreover, the asymmetry tensor orientation is given by: $K = \frac{3(\sigma_{iso}-\sigma_{22})}{\Omega}$

($-1 \leq K \leq +1$) in some cases of an axially symmetric tensor, (($-1 \leq \eta \leq +1$) will be zero, and hence, $\eta = 0$. However, the asymmetry (η) indicates how great deviation can appear from an axially symmetric tensor, therefore the region is $-1 \leq \eta \leq +1$.

Based on experimental and theoretical methods and concepts in our previous work our approaches and calculation have been done [38-94].

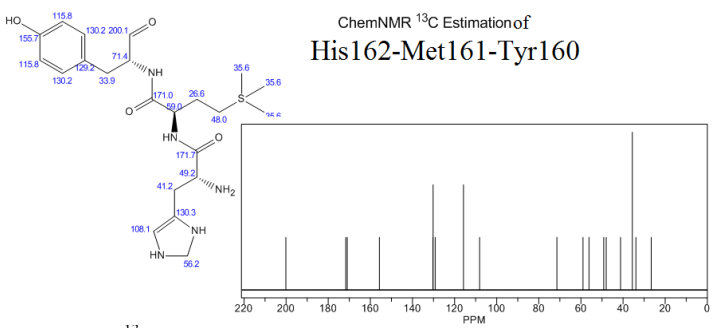

Figure 5. ^{13}CNMR data from B3LYP/6-31G**, for His162-Met161-Tyr160.

The most of proteins are localized at the site of intracellular trafficking, where it participates in CoV assembly and budding . Recombinant CoVs have lacking E exhibit significantly reduced viral tiers, crippled viral maturation, or yield propagation incompetent progeny, demonstrating the importance of E in virus production and maturation.

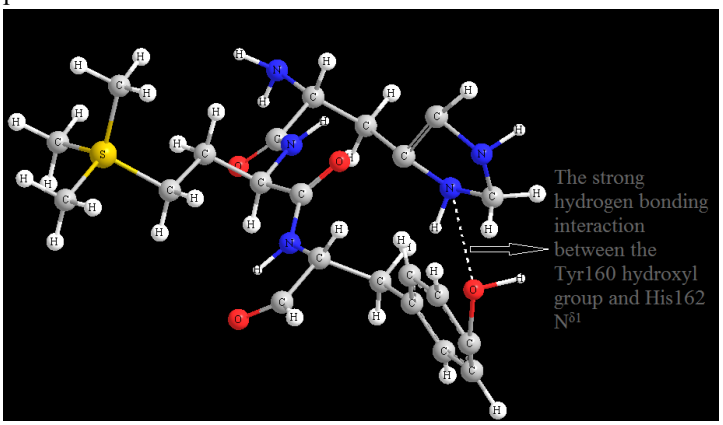

Figure 6. Optimized His162-Met161-Tyr160 through B3LYP/6-31G**, including the strong hydrogen bonding interaction between the Tyr160 hydroxyl group and His162 $N^{\delta 1}$.

A sub-regional analysis of both E and S revealed a triple cysteine motif located directly after the E protein TMD (NH2- … L-Cys-A-Y-Cys-Cys-N … -COOH) and a similar motif located in the C-terminus of S (NH2- … S-Cys-G-S-Cys-Cys-K … -COOH) . It can be supposed that the position and combination of these two motifs could serve as a structural basis for the association between E and S, which would be mediated by the formation of Disulphide bonds between the corresponding cysteine residues. Such evidence could also provide some insight into the debated topological conformations of the E protein .The presence of 10 methionine residues in the Covid-19 suggested that multi wave length anomalous dispersion could be used to solve the active site such as His162-Met161-Tyr160 (Figs5-7). The only exceptions were the two C-terminal residues which were not visible in five of the six chains.

2.2. Computational approaches.

The complex structures of several inhibitors have been done via dockings simulation. For docking with Vina [95], the receptor was processed with Auto dock Tools which water molecules have deleted and polar hydrogens and Gasteiger charges have been added in our model. Some necessary amino acids such as His were protonated in the neutral form accordance with crystal data. Our model of studies were chosen to be the tools

for testing the binding affinities of various natural products on beta-CoVs (SARS-CoV) and alpha (MERS-CoV) which are a basic virus for mutation towards COVID-19.

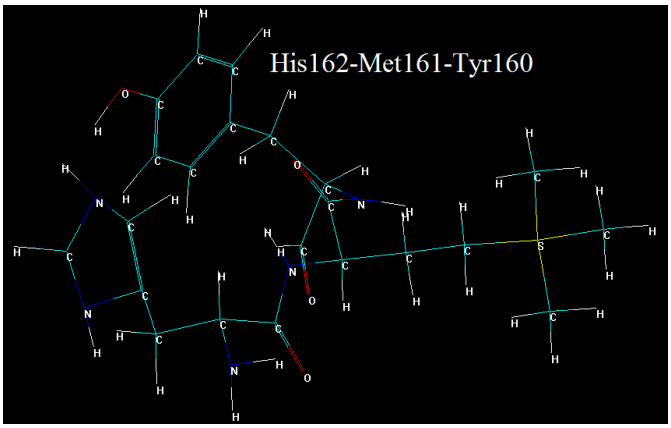

Figure 7. Active amino acids in COVID-19.

Sars-Cov2 (COVID-19) has several major proteins for producing its infection and growth, such as protease and spike glycoprotein. The RBD of spike (RBD-S) can bind to the ACE2 at PD of the host cell, consequently leading to a viral infection. In this work COVID-19 components compared to SARS-CoV-2. Computational calculation has been applied both by Linux and Windows 10 operating systems. Structure of 2019-nCoV chimeric receptor-binding domain complexed with its receptor human ACE2 of PDB ID 6VW1 [96] and COVID-19 main protease with un-landed active site (2019-nCoV, coronavirus disease 2019, SARS-CoV2) of PDB 6Y84 (Fig. 8).

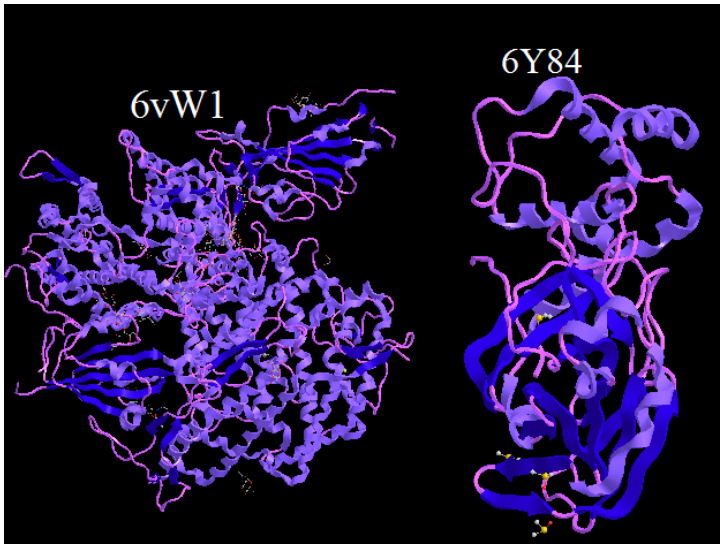

Figure 8. ACE2 of PDB ID 6VW1and COVID-19 main protease of PDB 6Y84

The PDB ID 6VW1 was applied as the model of PD-ACE2 in complex with RBD of covid-19. The molecular structure of all chemical components were extracted from drawn in Chemdraw, chemoffice and hyperchem software then subjected to conformational search and energy minimization in charmm with OPLS force fields. The docking simulation setting is also applied London dG and triangle matcher as score function of setting method. Several force fields such as Amber, MM+ and BIO+ were used parallel to OPLS for refining the docking results. Results of the molecular docking described the affinity represented by docking score and binding interaction of each compound on the protein target. ACE2 in human is an enzyme that has an effect on blood pressure. For COVID-19, ACE2 is a receptor, an entranceway, in the airways, alveolus and in blood vessel linings. ACE2 is also a receptor for β-CoV and NL63-CoV. It is notable that MERS-CoV or α- CoVs apply a different receptor. The way for developing vaccines and treatment is a 3-D figure of the parts of the virus that contact human cells. SARS and NL63-CoV bind to a helical part of ACE2 and attach with cell membranes via tunnels and bridges to comprise a “hot spot” for viruses.

The viral hot spot where beckons both SARS and COVID-19 is a shared drug and vaccine target – and so all the work on developing a SARS vaccine is now in the spotlight. Scientist from the S1 parts of the viral spikes hug the ACE2 receptor at a region of five amino acids to blocks the protein synthesize. Even though 4 or less amino acids differ in COVID-19, they are similar in size and charge to their counterparts in SARS. It is notable that S1 attaches SARS to the ACE2 receptor with docking. By this work we exhibited some molecules in Iranian natural product that help to removing the problem of COVID-19. Obviously the new virus “poses a significant public health risk for human transmission via the S-protein-ACE2 binding pathway.” The CoV covering has been done via (E) protein which is small, integrals protein consist of several aspects of the virus’ life cycle, such as assembling, enveloping, and formation. Although E protein is the smallest of the main structural proteins, the most important and enigmatic in viewo point of mechanism. During the replication cycle, E is translated much more numerous inside the infected cell.

2.3. Docking analysis.

In this work, Auto dock Tools and also iGEMDOCK software has been applied. Through this software, the acceptable receptor can be defined for the binding site in whole COVID-19 protein structures. The protein composition is worked with a ligand, and iGEMDOCK can helps to quickly define the suitable binding site. Following steps have been done in docking simulation :(a), Prepare Binding Site on the Protein Ligand. (b) Browsing and selecting the protein file. (c) Defining the binding site type as a bounded ligand. (d) Defining the center of the binding site by selected ligand. (e) Setting the size of the binding site through the extended radius from the selected ligand. IGEMDOCK yields an analysis surrounding with visualized tools and post-analysis tools for users which can be visualize the docked states, and categories through the protein-ligand interactions. Consequently, the prediction and scores of ligands can be saved in the output path. The minimum energies poses of each ligand will be outputted into the location of “best: Pose”.

These analysis tools are premeditated based on the analysis of those poses. Via looking for the bounded structures of some ligands, they can be select via the check box of ligand. If the co-crystallized ligands are retained on the binding site structures, it will be predicted poses. Cluster analysis is the partitioning of a data set into subsets. The data in each ideally subset will share some common trait. IGEMDOCK clusters the ligands based on interaction and atomic composition features. Interaction feature is extracted from the protein-ligand interactions and atomic

Composition is accounted atomic types in different functional groups. You are able to specify the number of cluster for your data or adjust the number by the preliminary clustered result. Cluster estimation is the analyzing of a data ranges into subsets. The information in each subset will share some general

properties. These are based on interaction and atomic combination aspects. Interaction aspects are extracted from the protein-ligand couples and atomic combinations are calculated atomic types in various functional groups.

3. RESULTS

In this decade, molecular modeling on the coronavirus of "S" has been simulated both the N-terminal and C-terminal regions (Scheme.2). S1 potentially can attach to host receptors as RBDs [97]. β- CoVs can be to bind proteinaceous receptor exclusively. The alpha coronavirus 229-E, serotype II feline CoV "F-CoV", and porcine respiratory CoVs apply the human aminopeptidase N of its host as receptor [98, 99].

The alpha corona virus and β-CoV or SARS-CoV both apply "ACE2" (Angiotensin converting enzyme 2) as a functional receptor [100], while the beta coronavirus and MERS-corona virus recruit "DPP4" (dipeptidyl peptidase-4) as a receptor (101, 102, and 103). RBMs mean "receptor-binding motifs" which in the S1 CTRs of α- CoVs and β-CoV spikes are demonstrated over a few loops from β-sheets structures [104, 105]. α- CoVs and β- CoV determine receptor specificity that might be varying extensively due to a similar core structure and common evolutionary origin. The identical positions are appearing for the CTRs of beta-CoVs SARS-CoV and alpha or MERS-CoV which bind ACE2 and DPP4, respectively [97].

In other hand, the CTRs of the alpha-Corona virus and H-CoV-NL-63 and beta-Corona virus SARS-CoV all recognize ACE2, through distinct molecular interactions [97]. The core CoV S Proteins structures of the CTRs in both α- CoVs and β-CoV prepare a scaffold from an extended loop(s) that might accommodate the receptor switching via exchange of the RBMs. The "NTR" of the alpha coronavirus and gamma coronavirus S proteins binds to sialic acids [106], while the NTR of β-CoV concluding B-CoV and H-CoVOC43 were exhibited for binding to O-acetylated sialic acids [107,108]. Only the NTR of subunit A is known for interacting with the protein receptors, being mCEACAM1a, while lacking any detectable sialic acid binding activity [109].

The NTR (MHV) exhibits a β-sandwich folding with family of sugar-binding proteins that probably have evolved from sugar-binding domains. The RBDs in different subunits of the S proteins which can bind either proteinaceous or glycan receptors illustrates a functional modularity of these glycoproteins at different subunits that might fulfill the role of binding to cellular attachment. The coronavirus S proteins are thought to have evolved from the basic structure receptor recognition which was confined to the CTR within S1.

The observed deletions of the NTR in some CoV species in nature are indicative of a less stringent requirement and integration of this domain with other regions of the spike trimer compared to the more C-terminally located domains of S1 and supports a scenario in which the NTR has been acquired at a later time point in CoV evolutionary history. Acquisition of glycan-binding domains and fusion thereof to the ancestral S protein may have resulted in a great extension of CoV host range and may have caused an increase in CoV diversity.

3.1. Discussion.

Among the herbal medicine that commonly used in relieving diseases we choose 4 species as the source for active constituents to be examined as its potential as anti SARS-CoV-2, namely *Matrine, Cytarabine, Gemcitabine and Vidarabine* from which are extracted from Gilan 's plants such as Trshvash, Chuchaq, Cote D'Couto and Khlvash in Iran. We used several representative compounds of each plant which are known to have pharmacological benefits (Fig.9). These plants are also believed to contribute for health and immune system among Iran people in relation to those of the active constituents.

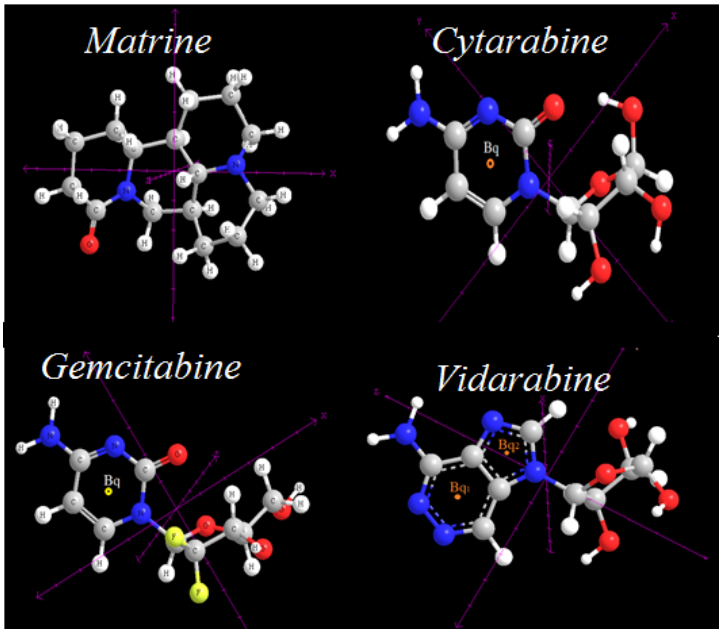

Figure 9. Chemical optimized structures of Matrine, Cytarabine, Gemcitabine and Vidarabine with M06 and m06-L (DFT) functional /cc-pvdz & cc-pvtz basis sets including NMR=CSGT including Pop=ChelpG

We applied molecular docking with 3 kind receptors; receptor human ACE2 of PDB ID 6VW1, 2019-nCoV, coronavirus disease 2019, SARS-CoV2) of PDB 6Y84 and SARS-Coronavirus NSP12 bound to NSP7 and NSP8 co-factors of PDB ID 6NUR (for compared its data information to new virus of covid-19) that are believed to contribute in virus infection in comparison with the respected known ligand or drugs as references. The result showed that several compounds could bind finely to the target receptors at the expected sides' .Several Gibbs energy of binding energies calculated by the docking scores among those of the compounds and those of the receptors (Table 1).

Table 1. Docking score of natural compounds towards several potential binding domain of SARS-CoV-2 , Energy Gibbs (kcal/mol)

Plant source	Ligand	Domain 6NUR	6Y84	RBD-ACE2 (6VW1)
Chuchaq	*Cytarabine*	-7.23	-9.33	-8.35
Trshvash	*Matrine*	-8.32	-8.44	-7.15
Cote D'Couto	*Gemcitabine*	-5.33	-7.33	-6.40
Khlvash	*Vidarabine*	-6.35	-7.12	-6.22

Interestingly, we exhibited; these compounds accomplish superior binding affinities to each receptor. These higher binding affinities of those of compounds could be represent significantly of its stronger inhibitory activities to the viral infection. Our molecular modelling also exhibited that *Cytarabine*, a compound found in *Chuchaq*, and *Matrine* from *Trshvash*, bind to those

receptors with lower energies compared to the respected reference compounds. These finding indicated that both compounds possess better binding interaction and may inhibit the initial virus infection to the host cell.

In addition it might noted that the docking scores of all the interaction models are still lower than that of *Gemcitabine and Vidarabine* which can be considered to have comparable effect of those interaction models. We may include those of compounds as candidates for further development as anti COVID-19.

4. CONCLUSIONS

The most efficiency of the NTR and CTR for binding to, protein receptors might be related to their arrangement in the S protein trimer and S1, S2 subunits. In contrast to the CTR, which is located in the center of the S trimer, the NTR is more distally oriented. Although protein–glycan interaction usually has low affinity, the more distal orientation of subunit "A" permitted multivalent receptors interactions, thereby increasing activities. Interestingly, some coronavirus have been seen as the dual receptors which can bind via their NTR and CTR to glycan and protein receptors, respectively.

5. REFERENCES

1. Cui, J.; Li, F.; Shi, Z.L. Origin and evolution of pathogenic coronaviruses. *Nat. Rev. Microbiol*. **2019**, *17*, 181-192, https://doi.org/10.1038/s41579-018-0118-9.
2. John, S.E.; Tomar, S.; Stauffer, S.R.; Mesecar, A.D. Targeting zoonotic viruses: Structure-based inhibition of the 3C-like protease from bat coronavirus HKU4-The likely reservoir host to the human coronavirus that causes Middle East Respiratory Syndrome (MERS). *Bioorg. Med. Chem*. **2015**, *23*, 6036-6048, https://doi.org/10.1016/j.bmc.2015.06.039.
3. Santos, Y.M.; Barraza, S.J.; Wilson, M.W.; Agius, M.P.; Mielech, A.M.; Davis, N.M.; Baker, S.C.; Larsen, S.D.; Mesecar, A.D. X-ray Structural and Biological Evaluation of a Series of Potent and Highly Selective Inhibitors of Human Coronavirus Papain-like Proteases. *J.Med.Chem*. **2014**, *57*, 2393-2412, https://doi.org/10.1021/jm401712t.
4. Hilgenfeld, R. From SARS to MERS: crystallographic studies on coronaviral proteases enable antiviral drug design. *FEBS J*. **2014**, *281*,4085-4096
5. Sevajol, M.; Subissi, L.; Decroly, E.; Canard, B.; Imbert, I.; Insights into RNA synthesis, capping, and proofreading mechanisms of SARS-coronavirus. *Virus Res***. 2014**, *194*, 90–99, https://doi.org/10.1016/j.virusres.2014.10.008.
6. Lehmann, K.C.; Gulyaeva, A.; Zevenhoven-Dobbe, J.C..; Janssen, G.M.; Ruben, M.; Overkleeft, H.S.; van Veelen, P.A.; Samborskiy, D.V.; Kravchenko, A.A.; Leontovich, A.M.; Sidorov, I.A.; Snijder, E.J.; Posthuma, C.C.; Gorbalenya, A.E. Discovery of an essential nucleotidylating activity associated with a newly delineated conserved domain in the RNA polymerasecontaining protein of all nidoviruses. *Nucleic Acids Res*. **2015**, *43*, 8416–8434, https://doi.org/10.1093/nar/gkv838.
7. Peersen, O.B. Picornaviral polymerase structure, function, and fidelity modulation. *Virus Res*. **2017**, *234*, 4–20, https://dx.doi.org/10.1016%2Fj.virusres.2017.01.026.
8. Baez-Santos, Y.M.; Barraza, S.J.; Wilson, M.W.; Agius, M.P.; Mielech, A.M.; Davis, N.M.; Baker, S.C.; Larsen, S.D.; Mesecar, A.D. X-ray Structural and Biological Evaluation of a Series of Potent and Highly Selective Inhibitors of Human Coronavirus Papain-like Proteases. *J.Med.Chem*. **2014**, *57***,** 2393-2412, https://doi.org/10.1021/jm401712t.
9. Woo, P.C.Y.; Lau, S.K.P.; Lam, C.S.F.; Lau, C.C.Y.; Tsang, A.K.L.; Lau, J.H.N.; Bai, R.; Teng, J.L.L.; Tsang, C.C.C.; Wang, M.; Zheng, B.J.; Chan, K.H.; Yuen, K.Y. Discovery of seven novel mammalian and avian coronaviruses in the genus *Deltacoronavirus* supports bat coronaviruses as the gene source of *Alphacoronavirus* and *Betacoronavirus* and avian coronaviruses as the gene source of *Gammacoronavirus* and *Deltacoronavirus*. *J. Virol.* **2012**, *86,* 3995–4008, https://doi.org/10.1128/JVI.06540-11.
10. Su, S.S.; Wong, G.; Shi, W.; Liu, J.; Lai, A.C.K.; Zhou, J.; Liu, W.; Bi, Y.H.; Gao, G.F. Epidemiology, genetic recombination, and pathogenesis of coronaviruses. *Trends Microbiol.* **2016,** *24*, 490–502, https://doi.org/10.1016/j.tim.2016.03.003.
11. Simon, A.; Völz, S.; Höfling, K.; Kehl, A.; Tillman, R.; Müller, A.; Kupfer, B.; Eis-Hübinger, A.M.; Lentze, M.J.; Bode, U.; Schildgen, O. Acute life threatening event (ALTE) in an infant with human coronavirus HCoV-229E infection. *Pediatr. Pulmonol.* **2007**, *42*, 393–396, https://doi.org/10.1002/ppul.20595.
12. Morfopoulou, S.; Brown, V.; Davies, E.G.; Anderson, G.; Virasami, A.; Qasim, W.; Chong, V.; Hubank, M.; Plagnol, V.; Desforges, M.; Jacques, T.S.; Talbot, P.J.; Breuer, J. Human coronavirus OC43 associated with fatal encephalitis. *N. Engl. J. Med.* **2016**, *375,* 497–498, https://doi.org/10.1056/NEJMc1509458.
13. Mayer, K.; Nellessen, C.; Hahn-Ast, C.; Schumacher, M.; Pietzonka, S.; Eis-Hübinger, A.M.; Drosten, C.; Brossart, P.; Wolf, D. Fatal outcome of human coronavirus NL63 infection despite successful viral elimination by IFN-alpha in a patient with newly diagnosed ALL. *Eur. J. Haematol.* **2016**, *97,* 208–210, https://doi.org/10.1111/ejh.12744.
14. Al-Khannaq, M.N.; Ng, K.T.; Oong, X.Y.; Pang, Y.K.; Takebe, Y.; Chook, J.B.; Hanafi, N.S.; Kamarulzaman, A.; Tee, K.K. Molecular epidemiology and evolutionary histories of human coronavirus OC43 and HKU1 among patients with upper respiratory tract infections in Kuala Lumpur, Malaysia. *Virol. J.* **2016**, *13,* 33, https://doi.org/10.1186/s12985-016-0488-4.
15. Oong, X.Y.; Ng, K.T.; Takebe, Y.; Ng, L.J.; Chan, K.G.; Chook, J.B.; Kamarulzaman, A.; Tee, K.K. Identification and evolutionary dynamics of two novel human coronavirus OC43 genotypes associated with acute respiratory infections: Phylogenetic, spatiotemporal and transmission network analyses. *Emerg. Microbes Infect.* **2017**, *6,* https://dx.doi.org/10.1038%2Femi.2016.132.
16. Lau, S.K.P.; Lee, P.; Tsang, A.K.L.; Yip, C.C.Y.; Tse, H.; Lee, R. A.; So, L.Y.; Lau, Y.L.; Chan, K.H.; Woo, P.C.Y.; Yuen, K.Y. Molecular epidemiology of human coronavirus OC43 reveals evolution of different genotypes over time and recent emergence of a novel genotype due to natural recombination. *J. Virol.* **2011**, *85,* 11325–11337, https://doi.org/10.1128/JVI.05512-11.
17. Menachery, V.D.; Yount Jr., B.L.; Sims, A.C.; Debbink, K.; Agnihothram, S.S.; Gralinski, L.E.; Graham, R.L.; Scobey, T.; Plante, J.A.; Royal, S.R.; Swanstrom, J.; Sheahan, T.P.; Pickles, R.J.; Corti, D.; Randell, S.H.; Lanzavecchia, A.; Marasco, W. A.; Baric, R.S. SARS-likeWIV1-CoV poised for human emergence. *Proc. Natl. Acad. Sci. U.S.A.* **2016**, *113*, 3048–3053, https://doi.org/10.1073/pnas.1517719113.
18. Yang, Y.; Liu, C.; Du, L.Y.; Jiang, S.; Shi, Z.; Baric, R.S.; Li, F. Two mutations were critical for bat-to-human transmission of Middle East Respiratory Syndrome coronavirus. *J. Virol.* **2015**, *89*, 9119–9123, https://doi.org/10.1128/JVI.01279-15.

19. Park, Y.J.; Walls, A.C.; Wang, Z.; Sauer, M.; Li, W.; Tortorici, M.A.; Bosch, B.J.; DiMaio, F.D.; Veesler, D.; Seattle Structural Genomics Center for Infectious Disease (SSGCID), *Nat.Struct.Mol.Biol* **2019,** *26*, 1151-1157, https://doi.org/10.1038/s41594-019-0334-7.
20. Chan, F.J.; To, K.K.; Tse, H.; Jin, D.Y.; Yuen, K.Y. Interspecies transmission and emergence of novel viruses: lessons from bats and birds. *Trends Microbiol*. **2013**, *21*, 544–555, http://dx.doi.org/10.1016/j.tim.2013.05.005.
21. Racaniello, V.R.; Skalka, A.M.; Flint, J.; Rall, G.F. *Principles of Virology, Bundle.* American Society of Microbiology, Washington, DC, 2015; http://dx.doi.org/10.1128/9781555819521.
22. Bosch, B.J.; Van Der Zee, R.; de Haan, C.A.M.; Rottier, P.J.M. The coronavirus spike protein is a class I virus fusion protein: structural and functional characterization of the fusion core complex. *J. Virol*. **2003**, *77*, 8801–8811, https://doi.org/10.1128/jvi.77.16.8801-8811.2003.
23. Baker, K.A.; Dutch, R.E.; Lamb, R.A.; Jardetzky, T.S. Structural basis for paramyxovirus-mediated membrane fusion. *Mol. Cell* **1999.** *3*, 309–319, http://dx.doi.org/10.1016/S1097-2765(00)80458-X.
24. Bartesaghi, A.; Merk, A.; Borgnia, M.J.; Milne, J.L.S.; Subramaniam, S. Prefusion structure of trimeric HIV-1 envelope glycoprotein determined by cryo-electron microscopy. *Nat. Struct. Mol. Biol*. **2013**, *20*, 1352–1357, http://dx.doi.org/10.1038/nsmb.2711.
25. Lin, X.; Eddy, N.R.; Noel, J.K.; Whitford, P.C.; Wang, Q.; Ma, J.; Onuchic, J.N. Order and disorder control the functional rearrangement of influenza hemagglutinin. *Proc. Natl. Acad. Sci. U.S.A*. **2014,** *111*, 12049–12054, http://dx.doi.org/10.1073/pnas.1412849111.
26. Hofmann, H.; Hattermann, K.; Marzi, A.; Gramberg, T.; Geier, M.; Krumbiegel, M.; Kuate, S.; Klaus, U.; Niedrig, M.; Pohlmann, S. S protein of severe acute respiratory syndrome-associated coronavirus mediates entry into hepatoma cell lines and is targeted by neutralizing antibodies in infected patients. *J. Virol*. **2004,** *78*, 6134–6142, http://dx.doi.org/10.1128/JVI.78.12.6134-6142.2004.
27. Walls, A.C.; Tortorici, M.A.; Bosch, B.J.; Frenz, B.; Rottier, P.J.M.; DiMaio, F.; Fey, F.A.; Veesler, D. Cryo-electron microscopy structure of a coronavirus spike glycoprotein trimer. *Nature* **2016**, *531,* 114–117, http://dx.doi.org/10.1038/nature16988.
28. Kirchdoerfer, R.N.; Cottrell, C.A.; Wang, N.; Pallesen, J.; Yassine, H.M.; Turner, H.L.; Corbett, K.S.; Graham, B.S.; McLellan, J.S.; Ward, A.B. Pre-fusion structure of a human coronavirus spike protein. *Nature* **2016**, *531,* 118–121, http://dx.doi.org/10.1038/nature17200.
29. Reguera, J.; Santiago, C.; Mudgal, G.; Ordon, D.; Enjuanes, L.; Casasnovas, J.M. Structural bases of coronavirus attachment to host aminopeptidase N and its inhibition by neutralizing antibodies. *PLoS Pathog*. **2012**, *8*, e1002859, https://dx.doi.org/10.1371%2Fjournal.ppat.1002859.
30. Akimkin, V.; Beer, M.; Blome, S.; Hanke, D.; Hoper, D.; Jenckel, M.; Pohlmann, A.; New chimeric porcine coronavirus in swine feces, Germany, 2012. *Emerg. Infect. Dis.* **2016,** *22 (7)*, 1314–1315. http://dx.doi.org/10.3201/eid2207.160179.
31. Wu, K.; Li, W.; Peng, G.; Li, F. Crystal structure of NL63 respiratory coronavirus receptor-binding domain complexed with its human receptor. *Proc. Natl. Acad. Sci. U.S.A*. **2009***, 106*, 19970–19974, http://dx.doi.org/10.1073/pnas.0908837106.
32. Duquerroy, B.S.; Vigouroux, A.; Rottier, P.J.M.; Rey, F.A.; Berend, T., Bosch, J. Central ions and lateral asparagine/glutamine zippers stabilize the post-fusion hairpin conformation of the SARS coronavirus spike glycoprotein. *Virology* **2005**, *335*, 276–285, http://dx.doi.org/10.1016/j.virol.2005.02.022.
33. Gao, J.; Lu, G.; Qi, J.; Li, Y.; Wu, Y.; Deng, Y.; et al., Structure of the fusion core and inhibition of fusion by a heptad repeat peptide derived from the S protein of Middle East respiratory syndrome coronavirus. *J. Virol*. **2013**, *87*, 13134–13140, http://dx.doi.org/10.1128/JVI.02433-13.
34. Xu, Y.; Lou, Z.; Liu, Y.; Pang, H.; Tien, P.; Gao, G.F.; Rao, Z. Crystal structure of severe acute respiratory syndrome coronavirus spike protein fusion core. *J. Biol. Chem.* **2004**, *279*, 49414–49419, http://dx.doi.org/10.1074/jbc.M408782200.
35. Ou, X.; Zheng, W.; Shan, Y.; Mu, Z.; Dominguez, S.R.; Holmes, K.V.; Qian, Z. Identification of the fusion peptide-containing region in betacoronavirus spike glycoproteins. *J. Virol*. **2016**, *90*, 5586–5600, https://doi.org/10.1128/JVI.00015-16.
36. Lu, G.; Hu, Y.; Wang, Q.; Qi, J.; Gao, F.; Li, Y.; Zhang, Y.; Zhang, W.; Yuan, Y.; Bao, J.; Zhang, B.; Shi, Y.; Yan, J.; Gao, G.F. Molecular basis of binding between novel human coronavirus MERS-CoV and its receptor CD26. *Nature* **2013,** *500,* 227–231, http://dx.doi.org/10.1038/nature12328.
37. Lu, L.; Liu, Q.; Zhu, Y.; Chan, K.-H.; Qin, L.; Li, Y.; Wang, Q.; Chan, J.F.W.; Du, L.; Yu, F.; Ma, C.; Ye, S.; Yuen, K.Y.; Zhang, R.; Jiang, S. Structure-based discovery of middle east respiratory syndrome coronavirus fusion inhibitor. *Nat. Commun.* **2014,** *5,* http://dx.doi.org/10.1038/ncomms4067.
38. Monajjemi, M. Molecular vibration of dopamine neurotransmitter: a relation between its normal modes and harmonic notes. *Biointerface Research in Applied Chemistry*, **2019**, *9*, 3956-3962, https://doi.org/10.33263/BRIAC93.956962.
39. Mollaamin, F.; Monajjemi, M. DFT outlook of solvent effect on function of nano bioorganic drugs. *Physics and Chemistry of Liquids* **2012**, *50*, 596-604, https://doi.org/10.1080/00319104.2011.646444.
40. Mollaamin, F.; Gharibe, S.; Monajjemi, M. Synthesis of various nano and micro ZnSe morphologies by using hydrothermal method. *International Journal of Physical Sciences* **2011**, *6*, 1496-1500.
41. Monajjemi M. Graphene/(h-BN)*n*/X-doped raphene as anode material in lithium ion batteries (X = Li, Be, B AND N). *Macedonian Journal of Chemistry and Chemical Engineering* **2017**, *36*, 101–118, http://dx.doi.org/10.20450/mjcce.2017.1134.
42. Monajjemi, M. Cell membrane causes the lipid bilayers to behave as variable capacitors: A resonance with self-induction of helical proteins. *Biophysical Chemistry* **2015**, *207*, 114-127, https://doi.org/10.1016/j.bpc.2015.10.003.
43. Monajjemi, M. Study of CD5+ Ions and Deuterated Variants (CHxD(5-x)+): An Artefactual Rotation. *Russian Journal of Physical Chemistry A*, **2018,** *92***,** 2215-2226.
44. Monajjemi, M. Liquid-phase exfoliation (LPE) of graphite towards graphene: An ab initio study. *Journal of Molecular Liquids* **2017**, *230*, 461–472, https://doi.org/10.1016/j.molliq.2017.01.044.
45. Jalilian, H.; Monajjemi, M. Capacitor simulation including of X-doped graphene (X = Li, Be, B) as two electrodes and (h-BN)m (m = 1–4) as the insulator. *Japanese Journal of Applied Physics* **2015**, *54,* 085101-7.
46. Ardalan, T.; Ardalan, P.; Monajjemi, M. Nano theoretical study of a C 16 cluster as a novel material for vitamin C carrier. *Fullerenes Nanotubes and Carbon Nanostructures* **2014**, *22*, 687-708.
47. Mahdavian, L.; Monajjemi, M.; Mangkorntong, N. Sensor response to alcohol and chemical mechanism of carbon nanotube gas sensors *Fullerenes Nanotubes and Carbon Nanostructures* **2009***, 17*, 484-495, https://doi.org/10.1080/15363830903130044.
48. Monajjemi, M.; Najafpour, J. Charge density discrepancy between NBO and QTAIM in single-wall armchair carbon

nanotubes. *Fullerenes Nanotubes and Carbon Nano structures* **2014**, *22*, 575-594, https://doi.org/10.1080/1536383X.2012.702161.
49. Monajjemi, M.; Hosseini, M.S. Non bonded interaction of B16 N16 nano ring with copper cations in point of crystal fields. *Journal of Computational and Theoretical Nanoscience* **2013**, *10*, 2473-2477.
50. Monajjemi, M.; Mahdavian, L.; Mollaamin, F. Characterization of nanocrystalline silicon germanium film and nanotube in adsorption gas by Monte Carlo and Langevin dynamic simulation. *Bulletin of the Chemical Society of Ethiopia* **2008**, *22*, 277-286, https://doi.org/10.4314/bcse.v22i2.61299.
51. Lee, V.S.; Nimmanpipug, P.; Mollaamin, F.; Thanasanvorakun, S.; Monajjemi, M. Investigation of single wall carbon nanotubes electrical properties and normal mode analysis: Dielectric effects. *Russian Journal of Physical Chemistry A* **2009**, *83*, 2288-2296, https://doi.org/10.1134/S0036024409130184.
52. Mollaamin, F.; Najafpour, J.; Ghadami, S.; Akrami, M.S.; Monajjemi, M. The electromagnetic feature of B N H (x = 0, 4, 8, 12, 16, and 20) nano rings:Quantum theory of atoms in molecules/NMR approach. *Journal of Computational and Theoretical Nanoscience* **2014**, *11*, 1290-1298.
53. Monajjemi, M.; Mahdavian, L.; Mollaamin, F.; Honarparvar, B. Thermodynamic investigation of enolketo tautomerism for alcohol sensors based on carbon nanotubes as chemical sensors. *Fullerenes Nanotubes and Carbon Nanostructures* **2010**, *18,* 45-55, https://doi.org/10.1080/15363830903291564.
54. Monajjemi, M.; Ghiasi, R.; Seyed, S.M.A. Metal-stabilized rare tautomers: N4 metalated cytosine (M = Li , Na , K , Rb and Cs), theoretical views. *Applied Organometallic Chemistry* **2003**, *17*, 635-640, https://doi.org/10.1002/aoc.469.
55. Ilkhani, A.R.; Monajjemi, M. The pseudo Jahn-Teller effect of puckering in pentatomic unsaturated rings C AE , A=N, P, As, E=H, F, Cl.*Computational and Theoretical Chemistry* **2015**, *1074*,19-25, http://dx.doi.org/10.1016%2Fj.comptc.2015.10.006.
56. Monajjemi, M. Non-covalent attraction of B N and repulsion of B N in the B N ring: a quantum rotatory due to an external field. *Theoretical Chemistry Accounts* **2015**, *134*, 1-22, https://doi.org/10.1007/s00214-015-1668-9.
57. Monajjemi, M.; Naderi, F.; Mollaamin, F.; Khaleghian, M. Drug design outlook by calculation of second virial coefficient as a nano study. *Journal of the Mexican Chemical Society* **2012**, *56*, 207-211, https://doi.org/10.29356/jmcs.v56i2.323.
58. Monajjemi, M.; Bagheri, S.; Moosavi, M.S. Symmetry breaking of B2N(-,0,+): An aspect of the electric potential and atomic charges. *Molecules* **2015**, *20*, 21636-21657, https://doi.org/10.3390/molecules201219769.
59. Monajjemi, M.; Mohammadian, N.T. S-NICS: An aromaticity criterion for nano molecules. *Journal of Computational and Theoretical Nanoscience* **2015**, *12*, 4895-4914, https://doi.org/10.1166/jctn.2015.4458.
60. Monajjemi, M.; Ketabi, S.; Hashemian, Z.M.; Amiri, A. Simulation of DNA bases in water: Comparison of the Monte Carlo algorithm with molecular mechanics force fields. *Biochemistry (Moscow)* **2006**, *71*, 1-8, https://doi.org/10.1134/s0006297906130013.
61. Monajjemi, M.; Lee, V.S.; Khaleghian, M.; Honarparvar, B.; Mollaamin, F. Theoretical Description of Electromagnetic Nonbonded Interactions of Radical, Cationic, and Anionic NH2BHNBHNH2 Inside of the B18N18 Nanoring. *J. Phys. Chem C* **2010**, *114*, 15315, https://doi.org/10.1021/jp104274z.
62. Monajjemi, M.; Boggs, J.E. A New Generation of BnNn Rings as a Supplement to Boron Nitride Tubes and Cages. *J. Phys. Chem. A* **2013**, *117*, 1670-1684, http://dx.doi.org/10.1021/jp312073q.
63. Monajjemi, M. Non bonded interaction between BnNn (stator) and BN B (rotor) systems: A quantum rotation in IR region. *Chemical Physics* **2013**, *425*, 29-45, https://doi.org/10.1016/j.chemphys.2013.07.014.
64. Monajjemi, M.; Robert, W.J.; Boggs, J.E. NMR contour maps as a new parameter of carboxyl's OH groups in amino acids recognition: A reason of tRNA–amino acid conjugation. *Chemical Physics* **2014**, *433*, 1-11, https://doi.org/10.1016/j.chemphys.2014.01.017.
65. Monajjemi, M. Quantum investigation of non-bonded interaction between the B15N15 ring and BH2NBH2 (radical, cation, and anion) systems: a nano molecularmotor. *Struct Chem* **2012,** *23*, 551–580, http://dx.doi.org/10.1007/s11224-011-9895-8.
66. Monajjemi, M. Metal-doped graphene layers composed with boron nitride–graphene as an insulator: a nano-capacitor. *Journal of Molecular Modeling* **2014**, *20*, 2507, https://doi.org/10.1007/s00894-014-2507-y.
67. Mollaamin, F.; Monajjemi, M.; Mehrzad, J. Molecular Modeling Investigation of an Anti-cancer Agent Joint to SWCNT Using Theoretical Methods. *Fullerenes nanotubes and carbon nanostructures* **2014**, *22*, 738-751, https://doi.org/10.1080/1536383X.2012.731582.
68. Monajjemi, M.; Ketabi, S.; Amiri, A. Monte Carlo simulation study of melittin: protein folding and temperature ependence, *Russian journal of physical chemistry* **2006**, *80,* S55-S62, https://doi.org/10.1134/S0036024406130103.
69. Monajjemi, M; Heshmata, M; Haeria, H.H. QM/MM model study on properties and structure of some antibiotics in gas phase: Comparison of energy and NMR chemical shift. *Biochemistry-moscow* **2006**, *71,* S113-S122 https://doi.org/10.1134/S0006297906130190.
70. Monajjemi, M.; Afsharnezhad, S.; Jaafari, M.R.; Abdolahi, A.N.; Monajemi, H. NMR shielding and a thermodynamic study of the effect of environmental exposure to petrochemical solvent on DPPC, an important component of lung surfactant. *Russian journal of physical chemistry A* **2007**, *81,* 1956-1963, https://doi.org/10.1134/S0036024407120096.
71. Mollaamin, F.; Noei, M.; Monajjemi, M.; Rasoolzadeh, R. Nano theoretical studies of fMet-tRNA structure in protein synthesis of prokaryotes and its comparison with the structure of fAla-tRNA. *African journal of microbiology research* **2011**, *5,* 2667-2674, https://doi.org/10.5897/AJMR11.310.
72. Monajjemi, M.; Heshmat, M.; Haeri, H. H.; et al. Theoretical study of vitamin properties from combined QM-MM methods: Comparison of chemical shifts and energy. *Russian journal of physical chemistry* **2006**, *80,* 1061-1068, https://doi.org/10.1134/S0036024406070119.
73. Monajjemi, M; Chahkandi, B. Theoretical investigation of hydrogen bonding in Watson-Crick, Hoogestein and their reversed and other models: comparison and analysis for configurations of adenine-thymine base pairs in 9 models. *Journal of molecular structure-theochem* **2005**, *714,* 43-60, https://doi.org/10.1016/j.theochem.2004.09.048.
74. Monajjemi, M.; Honarparvar, B.; Haeri, H.H.; Heshmat, M. An ab initio quantum chemical investigation of solvent-induced effect on N-14-NQR parameters of alanine, glycine, valine, and serine using a polarizable continuum model. *Russian journal of physical chemistry* **2006**, *80*, S40-S44, https://doi.org/10.1134/S0036024406130073.
75. Monajjemi, M.; Seyed Hosseini, M. Non Bonded Interaction of $B_{16}N_{16}$ Nano Ring with Copper Cations in Point of Crystal Fields. *Journal of Computational and Theoretical Nanoscience* **2013**, *10*, 2473-2477.
76. Monajjemi, M.; Farahani, N.; Mollaamin, F. Thermodynamic study of solvent effects on nanostructures: phosphatidylserine and phosphatidylinositol membranes. *Physics*

and chemistry of liquids **2012**, *50,* 161-172, https://doi.org/10.1080/00319104.2010.527842.
77. Monajjemi, M.; Ahmadianarog, M. Carbon Nanotube as a Deliver for Sulforaphane in Broccoli Vegetable in Point of Nuclear Magnetic Resonance and Natural Bond Orbital Specifications. *Journal of computational and theoretical nanoscience* **2014**, *11,* 1465-1471, https://doi.org/10.1166/jctn.2014.3519.
78. Monajjemi, M.; Ghiasi, R.; Ketabi, S.; Passdar, H.; Mollaamin, F. A Theoretical Study of Metal-Stabilised Rare Tautomers Stability: N4 Metalated Cytosine (M=Be^{2+}, Mg^{2+}, Ca^{2+}, Sr^{2+} and Ba^{2+}) in Gas Phase and Different Solvents. *Journal of Chemical Research* **2004**, *1*, 11-18, https://doi.org/10.3184/030823404323000648.
79. Monajjemi, M.; Baei, M.T.; Mollaamin, F. Quantum mechanic study of hydrogen chemisorptions on nanocluster vanadium surface. *Russian journal of inorganic chemistry* **2008**, *53,* 1430-1437, https://doi.org/10.1134/S0036023608090143.
80. Mollaamin, F.; Baei, M.T.; Monajjemi, M.; Zhiani, R.; Honarparvar, B. A DFT study of hydrogen chemisorption on V (100) surfaces. *RUSSIAN JOURNAL OF PHYSICAL CHEMISTRY A* **2008**, *82,* 2354-2361, https://doi.org/10.1134/S0036024408130323.
81. Monajjemi, M.; Honarparvar, B.; Nasseri, S.M.; Khaleghian, M. NQR and NMR study of hydrogen bonding interactions in anhydrous and monohydrated guanine cluster model: A computational study. *Journal of structural chemistry* **2009**, *50,* 67-77, https://doi.org/10.1007/s10947-009-0009-z.
82. Monajjemi, M.; Aghaie, H.; Naderi, F. Thermodynamic study of interaction of TSPP, CoTsPc, and FeTsPc with calf thymus DNA. *Biochemistry-Moscow* **2007**, *72,* 652-657, https://doi.org/10.1134/S0006297907060089.
83. Monajjemi, M.; Heshmat, M.; Aghaei, H.; Ahmadi, R.; Zare, K. Solvent effect on N-14 NMR shielding of glycine, serine, leucine, and threonine: Comparison between chemical shifts and energy versus dielectric constant. *Bulletin of the chemical society of ethiopia* **2007**, *21*, 111-116, https://doi.org/10.4314/bcse.v21i1.61387.
84. Monajjemi, M.; Rajaeian, E.; Mollaamin, F.; Naderi, F.; Saki, S. Investigation of NMR shielding tensors in 1,3 dipolar cycloadditions: solvents dielectric effect. *Physics and chemistry of liquids* **2008**, *46*, 299-306, https://doi.org/10.1080/00319100601124369.
85. Mollaamin, F.; Varmaghani, Z.; Monajjemi, M. Dielectric effect on thermodynamic properties in vinblastine by DFT/Onsager modelling. *Physics and chemistry of liquids* **2011,** *49,* 318-336, https://doi.org/10.1080/00319100903456121.
86. Monajjemi, M.; Honaparvar, B.; Hadad, B.K.; Ilkhani, A.R.; Mollaamin, F. Thermo-chemical investigation and NBO analysis of some anxileotic as Nano-drugs. *African journal of pharmacy and pharmacology* **2010**, *4,* 521-529.
87. Monajjemi, M.; Khaleghian, M.; Mollaamin, F. Theoretical study of the intermolecular potential energy and second virial coefficient in the mixtures of CH4 and Kr gases: a comparison with experimental data. *Molecular simulation* **2010**, *11,* 865-870, https://doi.org/10.1080/08927022.2010.489557.
88. Monajjemi, M.; Khosravi, M.; Honarparvar, B.; Mollamin, F. Substituent and Solvent Effects on the Structural Bioactivity and Anticancer Characteristic of Catechin as a Bioactive Constituent of Green Tea. *International journal of quantum chemistry* **2011**, *111,* 2771-2777, https://doi.org/10.1002/qua.22612.
89. Tahan, A.; Monajjemi, M. Solvent Dielectric Effect and Side Chain Mutation on the Structural Stability of Burkholderia cepacia Lipase Active Site: A Quantum Mechanical/ Molecular Mechanics Study. *Biotheoretica* **2011**, *59*, 291-312, https://doi.org/10.1007/s10441-011-9137-x.
90. Monajjemi, M.; Khaleghian, M. EPR Study of Electronic Structure of [CoF6](3-)and B18N18 Nano Ring Field Effects on Octahedral Complex. *Journal of cluster science* **2011**, *22*, 673-692, https://doi.org/10.1007/s10876-011-0414-2.
91. Monajjemi, M; Mollaamin, F. Molecular Modeling Study of Drug-DNA Combined to Single Walled Carbon Nanotube, *Journal of cluster science* **2012**, *23*, 259-272, https://doi.org/10.1007/s10876-011-0426-y.
92. Mollaamin, F; Monajjemi, M. Fractal Dimension on Carbon Nanotube-Polymer Composite Materials Using Percolation Theory. *Journal of computational and theoretical nanoscience* **2012**, *9*, 597-601, https://doi.org/10.1166/jctn.2012.2067.
93. Mahdavian, L.; Monajjemi, M. Alcohol sensors based on SWNT as chemical sensors: Monte Carlo and Langevin dynamics simulation. *Microelectronics journal* **2010**, *41,* 142-149, https://doi.org/10.1016/j.mejo.2010.01.011.
94. Monajjemi, M.; Falahati, M.; Mollaamin, F. Computational investigation on alcohol nanosensors in combination with carbon nanotube: a Monte Carlo and ab initio simulation. *Ionics* **2013**, *19*, 155-164, https://doi.org/10.1007/s11581-012-0708-x.
95. Huey, R.; Morris, G. *AutoDock Tools*; The Scripps Research Institute: La Jolla, CA, USA, 2003.
96. Shang, J.; Ye, G.; Shi, K.; Wan, Y.S.; Aihara, H.; Li, F.Structural basis for resptor recognition by novel coronavirus from wuhan, *Structural biology virology* **2020**, 03-04 ,DOI, 10.21203/rs.2.24749/v1
97. Li, F. Receptor recognition mechanisms of coronaviruses: a decade of structural studies. *J. Virol*. **2015**, *89*, 1954–1964, http://dx.doi.org/10.1128/JVI.02615-14.
98. Bonavia, A.; Zelus, B.D.; Wentworth, D.E.; Talbot, P.J.; Holmes, K.V. Identification of a receptor-binding domain of the spike glycoprotein of human coronavirus HCoV-229E. *J. Virol.* **2003**, *77*, 2530–2538, http://dx.doi.org/10.1128/JVI.77.4.2530-2538.2003.
99. Reguera, J.; Santiago, C.; Mudgal, G.; Ordono, D.; Enjuanes, L.; Casasnovas, J.M. Structural bases of coronavirus attachment to host aminopeptidase N and its inhibition by neutralizing antibodies. *PLoS Pathog.* **2012,** *8,* http://dx.doi.org/10.1371/journal.ppat.1002859.
100. Li, W.; Zhang, C.; Sui, J.; Kuhn, J.H.; Moore, M.J.; Luo, S.; Wong, S.K.; Huang, I.C.; Xu, K.; Vasilieva, N.; Murakami, A.; He, Y.; Marasco, W.A.; Guan, Y.; Choe, H.; Farzan, M. Receptor and viral determinants of SARS-coronavirus adaptation to human ACE2. *Embo J.* **2005**, *24,* 1634–1643, http://dx.doi.org/10.1038/sj.emboj.7600640.
101. Lu, G.; Hu, Y.; Wang, Q., Qi, J.; Gao, F.; Li, Y.; Zhang, Y.; Zhang, W.; Yuan, Y.; Bao, J.; Zhang, B.; Shi, Y.; Yan, J,l Gao, G.F. Molecular basis of binding between novel human coronavirus MERS-CoV and its receptor CD26. *Nature* **2013**, *500*, 227–231, http://dx.doi.org/10.1038/nature12328.
102. Mou, H.; Raj, V.S.; van Kuppeveld, F.J.M.; Rottier, P.J.M.; Haagmans, B.L.; Bosch, B.J. The receptor binding domain of the new Middle East respiratory syndrome coronavirus maps to a 231-residue region in the spike protein that efficiently elicits neutralizing antibodies. *J. Virol*. **2013**, *87*, 9379–9383, http://dx.doi.org/10.1128/JVI.01277-13.
103. Raj, V.S.; Mou, H.; Smits, S.L.; Dekkers, D.H.W.; Muller, M.A., Dijkman, R.; Muth, D.; Demmers, J.A.A.; Zaki, A.; Fouchier, R.A.M.; Thiel, V.; Drosten, C.; Rottier, P.J.M.; Osterhaus, A.D.M.E.; Bosch, B.J.; Haagmans, B.L. Dipeptidyl peptidase 4 is a functional receptor for the emerging human coronavirusEMC. *Nature* **2013**, *495*, 251–254, http://dx.doi.org/10.1038/nature12005.
104. Yang, Y.; Du, L.; Liu, C.; Wang, L.; Ma, C.; Tang, J.; Baric, R.S.; Jiang, S.; Li, F. Receptor usage and cell entry of bat coronavirus HKU4 provide insight into bat-to-human

transmission of MERS coronavirus. *Proc. Natl. Acad. Sci. U.S.A.* **2014**, *111,* 12516–12521, http://dx.doi.org/10.1073/pnas.1405889111.
105. Yang, Y.; Liu, C.; Du, L.; Jiang, S.; Shi, Z.; Baric, R.S.; Li, F. Two mutations were critical for bat-to-human transmission of Middle East respiratory syndrome coronavirus. *J. Virol.* **2015**, *89,* 9119–9123, http://dx.doi.org/10.1128/JVI.01279-15.
106. Promkuntod, N.; van Eijndhoven, R.; de Vrieze, G.; Grone, A.; Verheije, M. Mapping of the receptor-binding domain and amino acids critical for attachment in the spike protein of avian coronavirus infectious bronchitis virus. *Virology* **2014**, *448*, 26–32, http://dx.doi.org/10.1016/j.virol.2013.09.018.
107. Peng, G.; Sun, D.; Rajashankar, K.R.; Qian, Z.; Holmes, K.V.; Li, F. Crystal structure of mouse coronavirus receptor-binding domain complexed with its murine receptor. *Proc. Natl. Acad. Sci. U.S.A.* **2011**, *108,* 10696–10701.
108. Peng, G.; Xu, L.; Lin, Y.L.; Chen, L.; Pasquarella, J.R.; Holmes, K.V.; Li, F. Crystal structure of bovine coronavirus spike protein lectin domain. *J. Biol. Chem*. **2012**, *287*, 41931–41938, http://dx.doi.org/10.1074/jbc.M112.418210.
109. Langereis, M.A.; van Vliet, A.L.W.; Boot, W., de Groot; R.J. Attachment of mouse hepatitis virus to O-acetylated sialic acid is mediated by hemagglutinin-esterase and not by the spike protein. *J. Virol*. **2010**, *84,* 8970–8974, http://dx.doi.org/10.1128/JVI.00566-10.

6. ACKNOWLEDGEMENTS

The author thanks the Islamic Azad university, for providing the software and computer equipment.